A SINGLE-CHIP CMOS VISUAL ORIENTATION SENSOR

Reid R. Harrison

Department of Electrical and Computer Engineering
University of Utah
Salt Lake City, Utah 84112
harrison@ece.utah.edu

ABSTRACT

We present a single-chip, low-power vision sensor capable of measuring local edge orientation across a wide field of view. The sensor was fabricated in a 0.5-μm CMOS process. Quadratic spatial filters were implemented using differential pairs and an "antibump" circuit to give a current-mode output signal. Small spatial filters requiring only nearest-neighbor connectivity were used for edge detection. The sensor is able to detect its orientation relative to the dominant horizontal and vertical edges in indoor, man-made environments. This sensor consumes only 120 μW of power and could be used to control the attitude of an autonomous agent in an indoor environment.

1. INTRODUCTION

Small mobile platforms such as micro air vehicles (MAVs) require compact, low-power sensors to facilitate autonomous navigation. An important problem in aerial navigation is maintaining the proper attitude, or orientation with respect to the ground. Accelerometers may be used to sense the gravity vector, but this information is confounded with the self-acceleration inherent in flight.

In indoor man-made environments, vertical and horizontal edges dominate scenes, and diagonal edges are relatively rare. We propose that the dominance of horizontal and vertical edges could be used as a visual reference to determine attitude within a 90° range of uncertainty. A vision sensor that estimates local edge orientation over an extremely wide field of view could be used in concert with other sensors (i.e., accelerometers) to maintain correct attitude in a flying vehicle.

To estimate local edge orientation, we propose the use of quadratic spatial filters [1]. A simple quadratic filter has an output of the following form:

$$output = k \left(\sum_i w_i v_i \right)^2 \qquad (1)$$

Here, a number of input voltages v_i correspond to image intensity in a number of adjacent pixels. These intensity values are multiplied by a number of weights w_i, which represent the coefficients of an FIR spatial filter. In this work, we use spatial filters with a finite extent instead of diffusor-based spatial filtering techniques [2]. Filters resembling the oriented receptive fields observed in biological visual systems will return high magnitude responses to contrast edges, but the sign of the response will depend on the polarity of the edge. In other words, a black-to-white edge might elicit a strong positive response, while a white-to-black edge would elicit a strong negative response. To eliminate this sensitivity to edge polarity, we square the output of the linear filter, forcing all responses positive. A visual orientation sensor also employing oriented receptive fields, but not implementing a squaring operation, was reported in [3].

In this paper, we present a low-power, single-chip CMOS vision sensor capable of measuring local edge orientation across a wide field of view. We demonstrate that this sensor could be used to control the attitude of an autonomous agent in an indoor environment.

2. CIRCUIT DESIGN

We designed a chip with integrated imaging and focal-plane analog computation. For photodetection, we use 28 μm × 28 μm well-substrate photodiodes connected to two diode-connected pFETs in series (see Fig. 1a). The resulting voltage for a photodiode current I_{photo} is given by

$$v_{photo} = \frac{2U_T}{\kappa} \ln \frac{I_{photo}}{I_0} \qquad (2)$$

where $U_T = kT/q$ is the thermal voltage, $\kappa \approx 0.7$ is the gate coupling coefficient, and I_0 is the subthreshold drain current at $V_{GS} = 0$ [4].

To detect local edge orientation, we use spatial filters with six photoreceptor inputs drawn from nine possible

photoreceptors. We restrict ourselves to a 3 × 3 grid so that only nearest-neighbor connectivity is required on the chip. Figs. 1b and 1c show two such filters tuned for vertical edges and edges tilted 30° to the right of vertical, respectively. Each filter consists of three positively-weighted inputs and three negatively-weighted inputs, with all weights having equal magnitude.

To build a quadratic filter, we must first convolve the filter impulse response with the image and then square the output of the filter. Given our six-input filters with equal magnitude weights, the desired response of our quadratic filter can be expressed as

$$I_{out} = k\left(v_{p1} + v_{p2} + v_{p3} - v_{n1} - v_{n2} - v_{n3}\right)^2 \qquad (3)$$

The circuit used to approximate this computation is shown in Fig. 1d. This spatial filtering circuit relies on the equal number of positive and negative weights in each filter to allow differential pairs to be used for the implicit subtraction. Positively- and negatively-weighted photoreceptor signals are paired in each nMOS differential pair. In our circuit, each differential pair is biased by a current I_1. In the general case, different currents could be used in each differential pair to implement unequal weights across the filter.

The drain currents of the differential pairs are summed into two currents: I_p and I_n. These currents represent a differential current-mode encoding of the linear component of the filter (assuming the differential input voltages are in the millivolt range). Diode-connected pFETs turn these currents into voltages $v_{p\text{-}tot}$ and $v_{n\text{-}tot}$. For small input voltages, the difference between these two voltages ΔV is proportional to the difference between Σv_{pi} and Σv_{pi}.

These voltages serve as inputs to a pMOS "antibump" circuit first proposed by Delbrück in 1993 [5]. As long as all transistors are operated in the subthreshold region, the output current of this circuit is given by

$$I_{out} = I_2\left(1 - \frac{1}{\dfrac{4}{S}\cosh^2\dfrac{\kappa\Delta V}{2U_T}}\right) \qquad (4)$$

Where $\Delta V = v_{p\text{-}tot} - v_{n\text{-}tot}$ and S is the given by the ratio of transistor W/L ratios between the "middle" and "outer" transistors shown in Fig. 1d:

$$S = \frac{(W/L)_{\text{middle}}}{(W/L)_{\text{outer}}} \qquad (5)$$

In our design, we used $(W/L)_{\text{outer}} = 1.8\ \mu\text{m}/4.2\ \mu\text{m}$ and $(W/L)_{\text{middle}} = 4.2\ \mu\text{m}/1.8\ \mu\text{m}$ for a ratio of $S = 5.4$.

Fig. 2 shows the set of spatial filters used for orientation detection in our chip. The "straight" filters are tuned for horizontal and vertical edges, which represent the sensor being properly aligned with respect to an indoor environment. The "left" and "right" filters are tuned to ±30° rotations of horizontal and vertical edges and thus represent error signals in an attitude control system.

To reduce the size of the pixels in our imaging array, we used only three filters out of the possible six in each pixel. We divided the filters into two sets – "set 1" and "set 2" – and alternated these filters in a checkerboard pattern across our array. We also modified these filter patterns at the extreme corners of our array to compensate for the distortion caused by the wide-angle optics used.
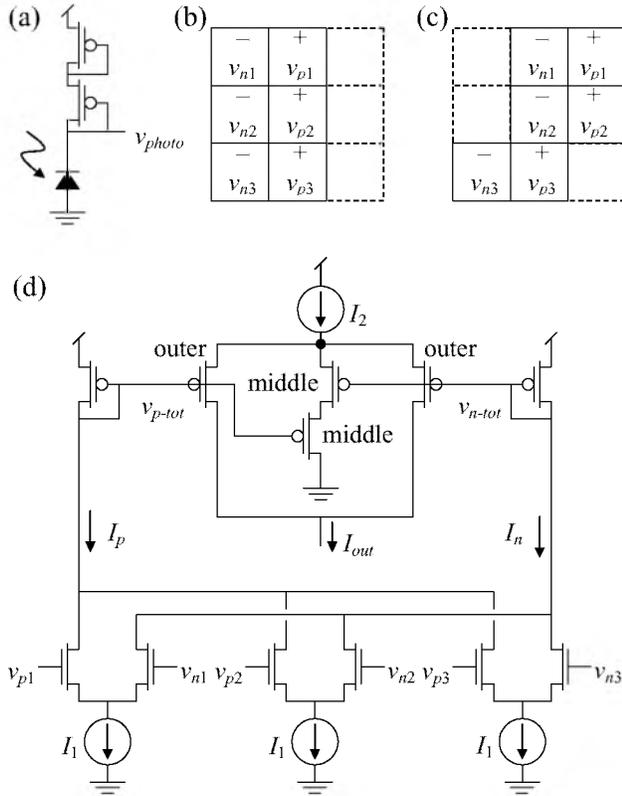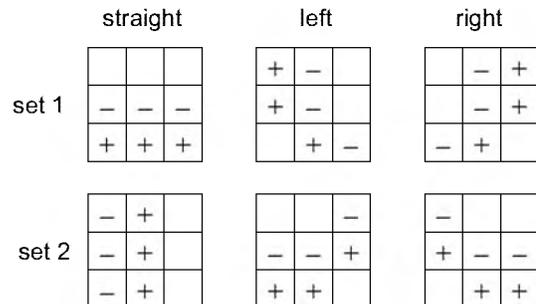

Figure 1: (a) Photoreceptor schematic. (b) Spatial filter tuned for vertical edges. (c) Spatial filter tuned for edges tilted 30° to the right of vertical. (d) Quadratic spatial filter circuit.

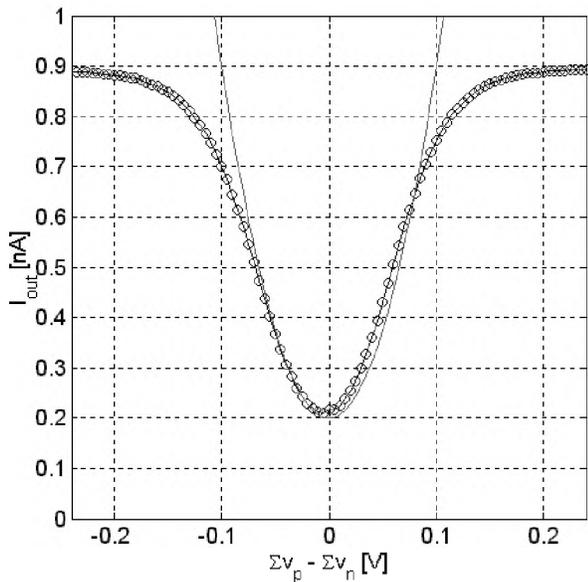Figure 2: Spatial filters used in orientation sensor.

Figure 3: Measured *I-V* response (circles) of quadratic spatial filter circuit from Fig. 1d.

Each pixel produced three current-mode signals – one for each orientation category: straight, left, or right. The output currents from each pixel were summed across the imaging array to produce three global output signals from the chip. We used off-chip transresistance amplifiers to convert the currents into three voltages we call $V_{straight}$, V_{left30}, and $V_{right30}$.

3. EXPERIMENTAL RESULTS

We fabricated a 20 × 20 pixel array in a 3-metal, 2-poly 0.5-μm CMOS process available through MOSIS. Each pixel measured 88 μm × 88 μm, resulting in a total array size of 1.76 mm × 1.76 mm. The total die size including pads was 2.24 mm × 2.24 mm. We used a single-polarity power supply of 5 V for all tests. Bias currents were set to $I_1 = 23$ nA and $I_2 = 0.90$ nA. (In order to keep the keep the I_2 current source in saturation, I_1 must be set much greater than I_2.) The chip consumes 120 μW of power.

The quadratic filter circuit was tested by applying a differential voltage to all three differential pairs (see Fig. 1d) and measuring the output current I_{out}. Fig. 3 shows the measured current as a function of input voltage (circles). The solid line shows an ideal quadratic function. For differential voltages less than ±80 mV, the circuit approximates the squared filter output with an additional offset current of 0.2 nA.

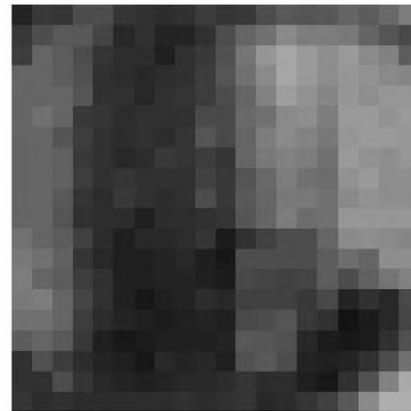**Figure 4:** Field of view used in experiment, as seen from digital camera.

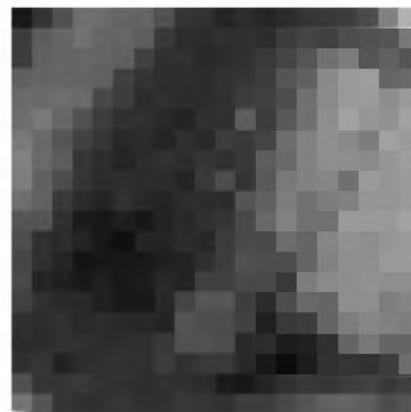**Figure 5:** Field of view from Fig. 4 as seen by the on-chip 20 × 20 photoreceptor array with θ = 0°.

Figure 6: Field of view from Fig. 4 as seen by the on-chip 20 × 20 photoreceptor array with θ = 30°.

IV - 946

We mounted a custom-built wide-angle lens over the chip. Our optics gave the chip an average field of view of 113° (101° from edge to edge, and 143° from corner to corner). The chip was mounted on a support that allowed it to be rotated to any angle θ.

The chip was oriented approximately 1 m above the ground, facing an office door. A high-resolution photograph corresponding to the chip's field of view was taken using a digital camera and fisheye lens attachment (Nikon Coolpix 995; Nikon FC-E8) and is shown in Fig. 4. The output from the chip's 20 × 20 photoreceptor array is shown in Fig. 5 for θ = 0° and Fig. 6 for θ = 30°.

The chip was rotated through a complete circle in 5° increments, and the summed output of the quadratic filters $V_{straight}$, V_{left30}, and $V_{right30}$ were recorded. We used off-chip op-amps to create the following voltages:

$$V_{sine}(\theta) = \frac{1}{\sqrt{3}}\left[V_{right30}(\theta) - V_{left30}(\theta)\right] \qquad (6)$$

$$V_{cosine}(\theta) = \frac{2}{3}\left[V_{straight}(\theta) - \frac{V_{right30}(\theta) + V_{left30}(\theta)}{2}\right] \qquad (7)$$

Figs. 7 and 8 show these measured voltages as the sensor was rotated through from θ = -180° to θ = +180°. Solid lines on both graphs show ideal fits to sin(4θ) (Fig. 7) and cos(4θ) (Fig. 8).

The "sine" response shown in Fig. 7 could be used as an error signal in a feedback system that stabilized the attitude of a flying vehicle, since this voltage goes to zero when the sensor is aligned with the dominant edges in the field of view (e.g., 0°, 90°). However, the "sine" response also goes to zero at intermediate angles (e.g., 45°), but in these cases the "cosine" signal could be used to disambiguate the true orientation angle.

4. CONCLUSIONS

We have presented a single-chip visual orientation sensor capable of measuring the dominate edge direction in an image. The chip is small and low power, consuming only 120 μW of power. This vision sensor could be used in concert with other sensors to maintain correct attitude in autonomous or semi-autonomous micro air vehicles. In this paper, we have demonstrated a forward-looking sensor that detects vertical angle. The sensor could also be positioned in an upward-looking configuration (using wide-angle optics) and be used to align a vehicle with respect to walls and corridors.

REFERENCES

[1] P. Perona and J. Malik, "Boundary detection using quadratic filters: performance criteria and experimental assessment," In: *Proc. SPIE Tech. Conf.*, Orlando, Fla., 1992.
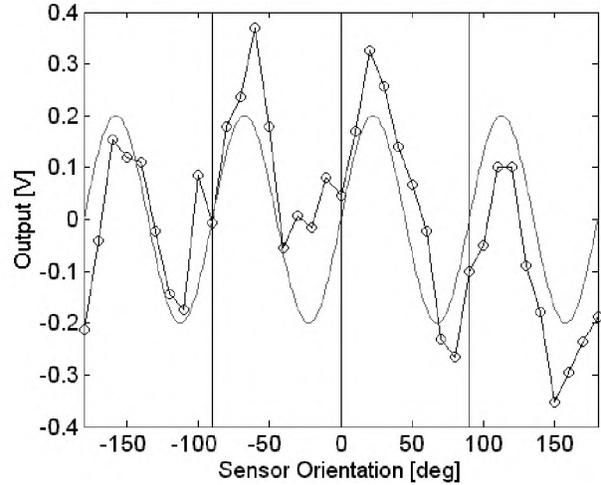
Figure 7: "Sine" response measured as sensor is rotated in a complete circle. Vertical lines show orientations of ±180°, ±90°, and 0°. Solid line is the function sin(4θ).

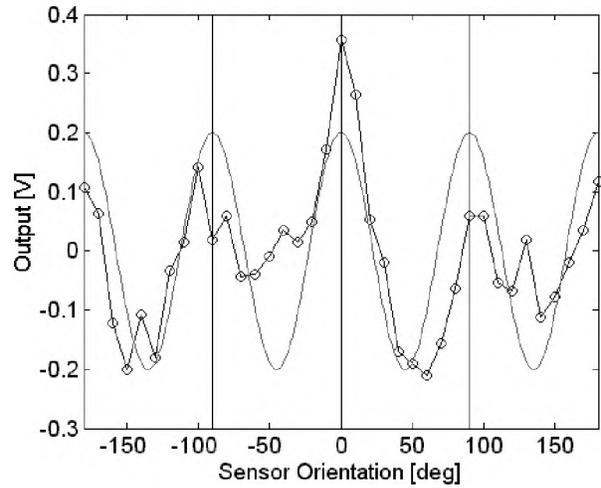**Figure 8:** "Cosine" response measured as sensor is rotated in a complete circle. Vertical lines show orientations of ±180°, ±90°, and 0°. Solid line is the function cos(4θ).

[2] A.G. Andreou and K.A. Boahen, "Translinear circuits in subthreshold MOS," *Analog Integrated Circuits and Signal Processing* 9:141-166, 1996.

[3] W.O. Camp and J. Van der Spiegel, "A silicon VLSI optical sensor for pattern recognition," *Sensors and Actuators A* 43:188-195, 1994.

[4] C. Mead, *Analog VLSI and Neural Systems*, Cambridge, MA: Addison-Wesley, 1989.

[5] T. Delbrück, "Bump circuits for computing similarity and dissimilarity of analog voltages," CNS Memo #26, California Institute of Technology, May 1993.